# Inlets for Waveriders Derived from Elliptic-Cone Stream Surfaces

Hamdi T. Hemdan* and Martin C. Jischke†
*University of Oklahoma, Norman, Oklahoma*

**The stream surfaces of the hypersonic flow of a gas past an elliptic cone are found in this paper and used to design blended inlets for waveriders. By perturbing the basic circular cone flow and stream surfaces for small values of $\epsilon$, where $\epsilon$ is a measure of the eccentricity of the elliptic cone, the stream surfaces of the elliptic-cone flow are found in closed form. Two arbitrary functions appear in the equation of the stream surface. By suitably choosing those functions, inlet shape can be controlled. Thus smooth, blended, symmetric designs are possible. The rate of mass flow through the inlet is found in closed form, and the effect of the various parameters on the shape of the inlet and the rate of mass flow is found and discussed in detail.**

## Nomenclature

$A_n$ = base area bounded by elliptic cone and shock
$\hat{e}_r, \hat{e}_\theta, \hat{e}_\phi$ = unit vectors in spherical polar coordinates
$K_\delta$ = hypersonic similarity parameter $= M_\infty \delta$
$\dot{m}$ = rate of mass flow through inlet
$r, \theta, \phi$ = spherical polar coordinates
$U, V, W$ = spherical velocity-component perturbations associated with elliptic cone
$u_0, v_0$ = radial and polar velocity component of the basic circular cone
$V_n$ = velocity normal to cone axis
$V\alpha, M_\infty$ = freestream velocity and Mach number
$\alpha$ = angle of attack
$\beta$ = circular-cone shock semivertex angle
$\gamma$ = ratio of specific heats
$\delta$ = semivertex angle of basic circular cone
$\epsilon$ = small parameter for cross-sectional eccentricity, Eq. (1)
$\lambda$ = elliptic-cone shock eccentricity factor
$\mu$ = constant $< 1$, Eq. (45)
$\xi_0$ = density ratio for basic shock, Eq. (3e)
$\rho$ = density
$\rho_\infty, \rho_s$ = density in the freestream and immediately behind the shock wave
$\Phi$ = function of $\phi$
$\phi^*$ = $\phi$ coordinate of the line of intersection of the inlet and the cone
$\nabla$ = differential operator

## I. Introduction

THE design of supersonic lifting bodies that produce maximum aerodynamic performance has received increasing attention over the past few years. This is due to the need for high-performance missiles and aircraft. Kuchemann[1] gives a detailed discussion of modern hypersonic aircraft needs and their design problems. Kuchemann recommends the use of stream surfaces of known flowfields as solid surfaces in a lifting-body configuration as a suitable method for providing the desired high performance. Normally the leading edges of such lifting-body configurations are sharp, yielding attached shock waves at leading edges. Lifting bodies designed this way are known as caret wings or waveriders.

Recently, Rasmussen[2,3] has proposed new waverider configurations derived from the flowfield past right elliptic cones at zero angle of attack and the flowfield past right circular cones at small angles of attack. Rasmussen's design of the waverider was attractive in the sense that it gave conical waveriders with smooth surface and sharp leading edges, and when experiments[4] were made on small models of his proposed waveriders, the elliptic-cone-derived waverider showed a high lift-to-drag ratio over a wide range of angles of attack. The shock wave formed below the lower surface was attached all along the leading edge for a wide range of the parameters.

The purpose of this work is to design inlets that can be attached to the waveriders derived by Rasmussen.[2,3] In principle, the analysis given here can be used for both the elliptic-cone and circular-cone waveriders derived by Rasmussen. However, this paper will be concerned with inlets for waveriders derived from elliptic cones at zero angle of attack only. Following the underlying principle used in the design of the waverider itself, we also take the solid surface of the inlet as a stream surface of the flowfield of the cone. This is consistent with the design of the waverider and should lead to high lift-to-drag configurations. That the inlet surface will be taken as a stream surface will not by itself assure a good design. The inlet surface needs to be smooth, with no sharp corners,‡ and symmetrically connected to the lower surface of the waverider. At the line (or curve) of intersection of the inlet with the waverider surface, the connection needs to be smooth, with the cone surface and the inlet surface having the same slope or slopes very close to each other. This helps minimize adverse heating effects. Inlets designed this way are known as blended inlets.

As a starting point, the flow past elliptic cones at zero angle of attack needs to be known. In this paper we shall be concerned with hypersonic flow only. The waverider analysis given in Refs. 2 and 3 is based on solutions given by Lee and Rasmussen[5] for hypersonic flow past right elliptic cones. In their work, following previous work,[6-8] Lee and Rasmussen sought the solution past the elliptic cone as a small perturbation of the known right-circular-cone flow. They then followed this straightforward perturbation solution with a further approximation that is valid for slender bodies in hyper-

Received March 25, 1985; revision received Feb. 8, 1986. 

*Visiting Assistant Professor; presently Assistant Professor, Mathematics Department, King Saud University, Riyadh, Saudi Arabia.

†Professor and Dean, College of Engineering; presently Chancellor, University of Missouri—Rolla, MO. Member AIAA.

‡Such sharp corners may arise if the inlet surface was made of two (or more) stream surfaces intersecting at an angle.

sonic flow. This approximation consists of expanding the perturbation equations in powers of a small parameter $\delta$, which characterizes the slenderness of the body, and neglecting second-order timers in $\delta$. The method gave simple closed-form results, which showed good agreement with experiment and other theories. However, this perturbtion solution was not uniformly valid in all the variables, and a thin vortical layer adjacent to the cone surface was present. In this vortical layer, entropy increases rapidly, making the straightforward perturbation solution singular at the cone surface. However, the simplicity of the method and the closed-form results obtained from it make it useful and very helpful, especially for preliminary design purposes, with which we are concerned in the present work.

It is important to recognize that the advantage of Lee and Rasmussen's theory—namely, that the results are obtained explicitly in closed form—was retained in Rasmussen's analysis of the waverider and in the present work. As we shall see later, it is possible to solve for the inlet surface shapes and for the associated mass flow rate in closed form.

In Sec. II, the stream surfaces of hypersonic flow past right elliptic cones at zero angle of attack will be found and then used to design blended inlets in Sec. III. The rate of mass flow through those inlets is found in Sec. IV. The paper ends with some concluding remarks and suggestions for future work.

## II. Stream Surfaces of Hypersonic Flow Past Elliptic Cones

Following the approach used to develop the waverider configuration, the inlet will be constructed from the stream surfaces of the ellitpic-cone flowfield. While the waverider was constructed using the conical stream surfaces that pass through the vertex of the cone, the inlet surface should not necessarily also be conical. It need only be a smooth symmetrical surface with no corners and blend smoothly into the cone surface.

Consider the hypersonic flow of a gas past a right elliptic cone of small eccentricity at zero angle of attack. The velocity components $u(\theta,\phi)$, $v(\theta,\phi)$ and $w(\theta,\phi)$ in spherical polar coordinates have been assumed in Ref. 5 in the form

$$\frac{u(\theta,\phi)}{V_\infty}=u_0(\theta)+\epsilon\cos2\phi U(\theta)+\ldots \tag{1a}$$

$$\frac{v(\theta,\phi)}{V_\infty}=v_0(\theta)+\epsilon\cos2\phi V(\theta)+\ldots \tag{1b}$$

$$\frac{w(\theta,\phi)}{V_\infty}=\epsilon\sin2\phi W(\theta)+\ldots \tag{1c}$$

$\rho$ and the pressure $p$ have also been found in Ref. 5, but they are not of interest in the present work. In the above representations, $\epsilon$ is a small parameter that characterizes the deviation of the elliptic-cone solution from that of a circular cone. The functions $u_0(\theta)$, $U(\theta)$, $v_0(\theta)$, $V(\theta)$, and $W(\theta)$, giving the approximate velocity components, will obviously be needed in this work. From Ref. 5 (Eqs. 5.2a, 5.2b, and 5.7–5.9), we get

$$u_0(\theta)\cong V_\infty[1+0(\delta^2)] \tag{2a}$$

$$v_0(\theta)=-\theta\left(1-\frac{\delta^2}{\theta^2}\right)V_\infty \tag{2b}$$

$$U(\theta)=\frac{X(\beta)}{\theta^2}+\frac{X'(\beta)}{4\beta^3\theta^2}(\theta^4-\beta^4)+\frac{1}{2}f_1\left[\sqrt{\frac{\theta^2-\delta^2}{\beta^2-\delta^2}}\left(\frac{5}{6}-\frac{\delta^2}{3\theta^2}\right)+\frac{\theta^2}{2\delta\sqrt{\beta^2-\delta^2}}\times\left(\cos^{-1}\frac{\delta}{\beta}-\cos^{-1}\right)\frac{\delta}{\theta}+\frac{\beta^2}{6\theta^2}+\frac{\delta^2}{3\theta^2}-1\right] \tag{2c}$$

$$V(\theta)=-\frac{2X(\beta)}{\theta^3}+\frac{1}{2}X'(\beta)\left(\frac{\theta}{\beta^3}+\frac{\beta}{\theta^3}\right)+f_1\left[\frac{1}{\theta}\sqrt{\frac{\theta^2-\delta^2}{\beta^2-\delta^2}}\left(\frac{1}{6}+\frac{\delta^2}{3\theta^2}\right)+\frac{\theta}{2\delta\sqrt{\beta^2-\delta^2}}\left(\cos^{-1}\frac{\delta}{\beta}-\cos^{-1}\frac{\delta}{\theta}\right)-\frac{\beta^2}{6\theta^3}-\frac{\delta^2}{3\theta^3}\right] \tag{2d}$$

$$W(\theta)=-\frac{2X(\beta)}{\theta^3}-\frac{X'(\beta)}{2\beta^3\theta^3}(\theta^4-\beta^4)-f_1\left[\frac{1}{\theta}\sqrt{\frac{\theta^2-\delta^2}{\beta^2-\delta^2}}\left(-\frac{1}{6}-\frac{\delta^2}{3\theta^2}\right)+\frac{\theta}{2\delta\sqrt{\beta^2-\delta^2}}\left(\cos^{-1}\frac{\delta}{\beta}-\cos^{-1}\frac{\delta}{\theta}\right)+\frac{\beta^2}{6\theta^3}+\frac{\delta^2}{3\theta^3}\right] \tag{2e}$$

where

$$\frac{\beta}{\delta}=\sigma=\sqrt{\frac{\gamma+1}{2}+\frac{1}{M_\infty^2\delta^2}} \tag{3a}$$

$$f_1=-2gV_\infty\beta(1-\xi_0)^2 \tag{3b}$$

$$X(\beta)=gV_\infty\beta^3(1-\xi_0) \tag{3c}$$

$$X'(\beta)=\frac{2}{(\gamma+1)}gV_\infty\beta^2[(\gamma-1)-\xi(\gamma+1)] \tag{3d}$$

$$\xi_0=1-\frac{\delta^2}{\beta^2} \tag{3e}$$

$$\frac{1}{\lambda}=\frac{1}{6\sigma^3}\left[\frac{3\cos^{-1}(1/\sigma)}{\sqrt{\delta^2-1}}+\frac{6}{(\gamma+1)}(\sigma^6+\sigma^2)+3\sigma^4-\sigma^2-5\right] \tag{3f}$$

Now, let the equation of a stream surface be given by

$$F(r,\theta,\phi)=0 \tag{4}$$

For $F=0$ to be a streamsurface, $F$ must satisfy the condition

$$V\cdot\nabla F=0 \tag{5}$$

where the velocity vector $V$ is given by

$$V=u\hat{e}_r+v\hat{e}_\theta+w\hat{e}_\phi$$

and $\hat{e}_r$, $\hat{e}_\theta$, and $\hat{e}_\phi$ are unit vectors in the $r$, $\theta$, and $\phi$ directions, respectively. $\nabla$ is the vector operator

$$\nabla=\frac{\partial}{\partial r}\hat{e}_r+\frac{1}{r}\frac{\partial}{\partial\theta}\hat{e}_\theta+\frac{1}{r\sin\theta}\frac{\partial}{\partial\phi}\hat{e}_\phi$$

Writing Eq. (5) in detail gives

$$ur\sin\theta\frac{\partial F}{\partial r}+v\sin\theta\frac{\partial F}{\partial\theta}+w\frac{\partial F}{\partial\theta}=0 \tag{6}$$

which is a first-order linear partial differential equation for the function $F$ and can be solved by the well-known theory of characteristics. In particular, a streamline is given by the simultaneous equations

$$\frac{dr}{u}=\frac{r\,d\theta}{v}=\frac{r\sin\theta\,d\phi}{w} \tag{7}$$

Let us now introduce the approximations made in Ref. 5 in the equation of the stream surface; i.e., assume that $F(r,\theta,\phi)$ can be expanded in the form

$$F(r,\theta,\phi)=\ell n r-f(\theta,\phi)-\epsilon g(\theta,\phi)+0(\epsilon^2)=0 \tag{8}$$

where $f(\theta,\phi)$ and $g(\theta,\phi)$ are unknown functions to be found. That the flowfield is conical is included in the above equation by taking the first term on the right-hand side as $\ell n r$ instead of $r$. We substitute the series expansion Eq. (8) and Eqs. (1) into Eq. (4) and equate like powers of $\epsilon$ to get the following two partial differential equations for the determination of the functions $f$, $g$:

$$v_0(\theta)\frac{\partial f}{\partial\theta}=1 \tag{9a}$$

$$v_0(\theta)\frac{\partial g}{\partial\theta}=\cos 2\phi\left[U(\theta)-V(\theta)\frac{\partial f}{\partial\theta}\right]-\frac{W(\theta)}{\theta}\sin 2\phi\frac{\partial f}{\partial\phi} \tag{9b}$$

In the preceding equations, it is seen that $\phi$ appears as a parameter rather than a variable; thus, the equations can be solved as ordinary differential equations and their solutions can be readily found as

$$f(\theta,\phi)=\ell n\frac{k(\phi)}{\sqrt{\theta^2-\delta^2}} \tag{10a}$$

$$g(\theta,\phi)=\cos 2\phi G(\theta)-\sin 2\phi\frac{k'(\phi)}{k(\phi)}H(\theta)+h(\phi) \tag{10b}$$

where $k(\phi)$ and $h(\phi)$ are arbitrary functions and $G(\theta)$ and $H(\theta)$ are given by

$$G(\theta)=\int\left(\frac{U(\theta)}{v_0(\theta)}-\frac{V(\theta)}{v_0(\theta)}\right)d\theta \tag{11a}$$

$$H(\theta)=\int\frac{W(\theta)}{\theta v_0(\theta)}d\theta \tag{11b}$$

The stream surface can thus be written in the form

$$\ell n r=\ell n\frac{k(\phi)}{\sqrt{\theta^2-\delta^2}}+\epsilon\left[\cos 2\phi G(\theta)-\sin 2\phi\frac{k'(\phi)}{k(\phi)}H(\theta)+h(\phi)\right] \tag{12}$$

Equation (12) gives the most general nonconical stream surface. The nonconicity results from the presence of $r$ in the equation. The simplest steam surface results from the choice of $k(\phi)$ and $h(\phi)$ as

$$k(\phi)=1, \qquad h(\phi)=0$$

This gives the surface

$$\ell n r\sqrt{\theta^2-\delta^2}-\epsilon\cos 2\phi G(\theta)=0 \tag{13}$$

Having found the nonconical stream surfaces, we proceed to find the conical ones. First, we mention that the conical stream surfaces have been found[2] using the equations of the streamline [Eq. (7)]. They can also be found through the present procedure by assuming that the function $F(r,\theta,\phi)$ is independent of $r$. Thus, let

$$F(r,\theta,\phi)\equiv F_1(\theta,\phi)$$

and, for the function $F_1(\theta,\phi)$, assume the series expansion

$$F_1(\theta,\phi)=\ell n\frac{\tan\phi}{\tan\phi_s}-2\epsilon\tilde{H}(\theta)+0(\epsilon^2)=0 \tag{14}$$

where $\phi_s$ is a constant and $\tilde{H}(\theta)$ is an unknown function to be determined. Now, substitute Eq. (12) into Eq. (5) and retain the lowest-order terms in $\epsilon$ to get

$$\tilde{H}(\theta)=\int\frac{W(\theta)}{\theta v_0(\theta)}d\theta \tag{15}$$

Comparing Eqs. (15) and (11b), we find that $\tilde{H}\equiv H(\theta)$. The result given by Eqs. (14) and (15) for the conical stream surface is the same as that found by solving the streamline equations.[2]

Once the functions $G(\theta)$ and $H(\theta)$ are found, both families of stream surfaces i.e., the conical and the nonconical stream surfaces, become known. The function $\tilde{H}(\theta)$ is found approximately[2] by replacing the function $W(\theta)$ by a simple two-term approximating function [see Eq. (17)]. We shall use the result of Ref. 2 because of its simplicity, although an exact evaluation of $\tilde{H}(\theta)$ could be made as is done in evaluating the function $F(\theta)$ next. Comparing Eq. (14) with Eq. (5-5) in Ref. 2, we find that

$$\tilde{H}(\theta)=\frac{1}{2}k_1\ell n\frac{\theta-\theta_c}{\theta_s^*-\theta_c}+\frac{1}{2}k_2\ell n\frac{\theta+\theta_c}{\theta_s^*+\theta_c}-\frac{1}{2}(k_1+k_2)\ell n\frac{\theta}{\theta_s^*} \tag{16}$$

where

$$\theta_c=\delta-\epsilon\cos 2\phi, \quad \theta_s^*=\beta-\epsilon\lambda\cos 2\phi$$

$$k_1=-\frac{1}{\delta}\frac{W(\delta)}{V_\infty}, \quad k_2=-\frac{1}{\delta}\left[\frac{(\sigma+1)W(\delta)-2\sigma W(\beta)}{(\sigma-1)V_\infty}\right]$$

$$W(\theta)=A+\frac{\theta_c}{\theta}B, \qquad A=\frac{\tilde{\sigma}W(\theta_s)-W(\theta_c)}{\sigma-1}$$

$$B=\frac{\tilde{\sigma}[W(\theta_c)-W(\theta_s)]}{\tilde{\sigma}-1}, \qquad \tilde{\sigma}=\sigma+0(\epsilon) \tag{17}$$

Equation (16) may also be written

$$H(\theta)=\tfrac{1}{2}k_1\ell n(\theta-\theta_c)+\tfrac{1}{2}k_2\ell n(\theta+\theta_c)-\tfrac{1}{2}(k_1+k_2)\ell n\theta \tag{18}$$

Equation (16) is to be used for the conical stream surfaces, i.e., in Eq. (14), while Eq. (18) is the be used for the nonconical stream surfaces [Eq. (12)]. The difference between the two equations is that the constant of integration is set equal to zero in Eq. (18).

We now proceed to find the function $G(\theta)$. From Eqs. (2b-d), the order of magnitude of the functions $U(\theta)$, $v_0(\theta)$ and $V(\theta)$ can be found to be

$$U(\theta)=0(\theta), \quad V(\theta)=0(1), \quad v_0(\theta)=0(\theta)$$

Using those orders of magnitude in Eq. (11a), we get

$$\frac{U(\theta)}{v_0(\theta)}=0(1), \quad \frac{V(\theta)}{v_0^2(\theta)}=0\left(\frac{1}{\theta^2}\right)$$

i.e., the function $V/v_0^2$ is two orders of magnitude larger than the function $U/v_0$. Therefore, the effect of $U/v_0$ on $G(\theta)$ can be neglected completely, and we can write

$$G(\theta)\simeq-\int\frac{V(\theta)}{v_0^2(\theta)}d\theta \tag{19}$$

In order to be able to evaluate the integral defining $G(\theta)$ in a closed form, the function $V(\theta)$ needs to be written in a more convenient form by making the following substitutions. Let

$$b_1 = -2X(\beta), \qquad b_2 = \frac{X'(\beta)}{2\beta^3}$$

$$b_3 = \frac{\beta X'(\beta)}{2}, \qquad b_4 = \frac{1}{\sqrt{\beta^2 - \delta^2}}$$

$$b_5 = \frac{\delta^2}{3}, \qquad b_6 = \frac{1}{2\delta\sqrt{\beta^2 - \delta^2}}$$

$$b_7 = \cos^{-1}\frac{\delta}{\beta}, \qquad b_8 = -\frac{\beta^2}{6} - \frac{\delta^2}{3} \tag{20}$$

Equation (2d) for $V(\theta)$ then becomes

$$V(\theta) = (b_1 + b_3 + f_1 b_8)\ \frac{1}{\theta^3} + (b_2 + f_1 b_6 b_7)\theta + \frac{1}{6} f_1 b_4 \frac{\sqrt{\theta^2 - \delta^2}}{\theta} + f_1 b_4 b_5 \frac{\sqrt{\theta^2 - \delta^2}}{\theta^3} - f_1 b_6 \theta \cos^{-1}\frac{\delta}{\theta}$$

Further, write

$$B_1 = b_1 + b_3 + f_1 b_8, \quad B_2 = b_2 + f_1 b_6 b_7$$

$$B_3 = \frac{1}{6} f_1 b_4, \qquad B_4 = f_1 b_4 b_5, \qquad B_5 = -f_1 b_6 \tag{21}$$

Finally, $V(\theta)$ takes the simple form

$$V(\theta) = \frac{B_1}{\theta^3} + B_2\theta + B_3\frac{\sqrt{\theta^2 - \delta^2}}{\theta} + B_4\frac{\sqrt{\theta^2 - \delta^2}}{\theta^3} + B_5\theta \cos^{-1}\frac{\delta}{\theta}$$

and $G(\theta)$ can be written as

$$G(\theta) = \int \left[\frac{B_1}{\theta(\theta^2 - \delta^2)^2} + \frac{B_2\theta^3}{(\theta^2 - \delta^2)^2} + \frac{B_3\theta}{(\theta^2 - \delta^2)^{3/2}} + \frac{B_4}{\theta(\theta^2 - \delta^2)^{3/2}} + \frac{B_5\theta^3 \cos^{-1}\delta/\theta}{(\theta^2 - \delta^2)^2}\right] d\theta \tag{22}$$

All the integrals in the right-hand side of Eq. (22) can be found in closed form. The final result is

$$G(\theta) = \frac{B_1}{2\delta^2}\left[\frac{1}{(\delta^2 - \theta^2)} + \frac{1}{\delta^2}\ln\frac{\theta^2}{(\theta^2 - \delta^2)}\right] + \frac{B_2}{2}\left[\frac{-\delta^2}{(\theta^2 - \delta^2)} + \ln(\theta^2 - \delta^2)\right] - \frac{B_3}{\sqrt{\theta^2 - \delta^2}} - \frac{B_4}{\delta^2}\left[\frac{1}{\sqrt{\theta^2 - \delta^2}} + \frac{1}{\delta}\cos^{-1}\frac{\delta}{\theta}\right] + B_5\left\{\eta\left[\ln(\tan\eta) - \frac{1}{2}\operatorname{cosec}^2\eta\right] - \frac{1}{2}\cot\eta - \eta\ln\eta + \eta - \frac{\eta^3}{9} - \frac{7}{450}\eta^5\right\} \tag{23}$$

where $\eta = \cos^{-1}(\delta/\theta)$. In evaluating the last integral in Eq. (22), it was assumed that $\cos^{-1}(\delta/\theta)$ is small and the integral was found as an infinite series in $\eta$, of which only the first four terms are retained and other higher-order terms were neglected. Those terms retained are the last four terms in Eq. (23). The assumption that $\eta$ is small is justified, since $\eta = 0$ at cone surface and its largest value at shock wave is always small for hypersonic flow. For example, when $\gamma = 1.4$ and $M_\infty\delta = 1.0$, we get from Eq. (3a) $\beta/\delta = 1.48$; thus $\eta = 0.83$, and when $\gamma = 1.4$, and $M_\infty\delta = 3$, $\beta/\delta = 1.145$, and $\eta = 0.51$.

Again, it is necessary to write Eq. (23) in its simplest form in order to be able to continue the process of solving in closed form. Thus, let us introduce the notations

$$A_1 = -\frac{B_1}{2\delta^2} - \frac{B_2\delta^2}{2} - \eta\theta B_5/2$$

$$A_2 = \frac{B_4}{\delta^2} - B_3 - \frac{\delta B_5}{2}$$

$$A_3 = \frac{B_2}{2} + \eta\frac{B_5}{2} - \frac{B_1}{2\delta^4}$$

Thus, we get

$$G(\theta) = \frac{A_1}{\theta^2 - \delta^2} + \frac{A_2}{\sqrt{\theta^2 - \delta^2}} + A_3\ln(\theta^2 - \delta^2) + A_4\ln\theta/\delta^4 - B_5\phi\ln\delta - B_4\eta/\delta^3 + B_5(\eta - \eta\ln\eta - \eta^3/9 - 7\eta^5/450) \tag{24}$$

Having found the functions $G(\theta)$ and $H(\theta)$, both of the conical and the nonconical stream surfaces are known; we are in a position to choose a suitable surface to make the solid boundary of the inlet. This is considered in the following section.

## III. Blended Inlets

In this section we use the stream surfaces found in the previous section to design a blended inlet. The basic requirement is that the surface be smooth and symmetric with respect to the plane $\phi = 0$. Corners must be avoided because of their potential for adverse heating effects. Also desirable is a smooth connection between the inlet and the cone. The slopes of the inlet surface and the cone surface need to be equal or close to each other at the curve of connection. This helps minimize adverse heating effects. As mentioned before, inlets having the same slope as the cone at the curve of intersection are known as blended inlets.

By squaring both sides of Eq. (12) and rearranging terms, the general stream surface may be written as

$$k^2(\phi) + 2\epsilon k(\phi)[k(\phi)h(\phi) - \sin 2\phi k'(\phi)H(\theta)] = r^2(\theta^2 - \delta^2)[1 - 2\epsilon\cos 2\phi G(\theta)] \tag{25}$$

We assume that the inlet surface can be made of one of the above surfaces. To find the cross section of the inlet with any plane $z = \text{const} = \ell_1$, where $0 < \ell_1 \le \ell$, and $\ell$ is the total length of the cone, we make the substitutions

$$r = \ell_1\cos\theta \approx \ell_1 \quad \text{and} \quad \theta = \Phi(\phi)$$

in Eq. (25). Thus, we get

$$k^2(\phi) + 2\epsilon k^2(\phi)h(\phi) - 2\epsilon\sin 2\phi k(\phi)k'(\phi)H[\Phi(\phi)] = \ell_1^2[\Phi^2(\phi) - \delta^2]\{1 - 2\epsilon\cos 2\phi G[\Phi(\phi)]\} \tag{26}$$

The unknown in Eq. (26) is the function $\Phi(\phi)$, which gives the cross section of the inlet with the plane $z=\text{const}=\ell_1$. The functions $k(\phi)$ and $h(\phi)$ are arbitrary and need to be chosen such that $\Phi(\phi)$ is a smooth, symmetric function having, if possible, the same slope as the cone surface at the points of intersection with the cone. It is to be noticed that Eq. (26) is a functional equation for $\Phi(\phi)$ whose solution in closed form does not seem to be possible. However, consistent with the perturbation approach used here, we assume that $\Phi(\phi)$ can be expanded in powers of $\epsilon$ in the form

$$\Phi(\phi)=\theta_0-\epsilon\cos2\phi\,\theta_1+0(\epsilon^2) \tag{27}$$

where $\theta_0(\phi)$ and $\theta_1(\phi)$ are unknown functions to be determined. Substituting Eq. (27) into Eq. (26) and equating like powers of $\epsilon$, we obtain $\theta_0(\phi)$ and $\theta_1(\phi)$ as

$$\theta_0(\phi)=\sqrt{\delta^2+\frac{k^2(\phi)}{\ell_1^2}} \tag{28}$$

$$\theta_1=\frac{1}{\theta_0(\phi)}\left\{-\frac{1}{\ell_1^2}\sec2\phi\;k^2(\phi)h(\phi)\right.$$
$$+\frac{1}{\ell_1^2}\tan2\phi k'(\phi)\sqrt{\theta_0^2(\phi)-\delta^2}H[\theta_0(\phi)]$$
$$\left.-[\theta_0^2(\phi)-\delta^2]G[\theta_0(\phi)]\right\} \tag{29}$$

Once the functions $k(\phi)$ and $h(\phi)$ are chosen, $\theta_0(\phi)$ and $\theta_1(\phi)$ become known. Beside the continuity and smoothness, the function $k(\phi)$ needs to satisfy the following requirements:

1) It is an even function, i.e., $k(\phi)=k(-\phi)$. This assures the symmetry of the inlet with respect to the plane $\phi=0$.

2) It is equal to zero for a certain value of $\phi$, say $\phi^*$, such that $0<\phi^*<\pi$. This assures the intersection between the inlet and the cone.

When $k(\phi)$ is chosen such that the above conditions are satisfied, then we get from Eq. (28):

$$\theta_0(\phi^*)=\delta \tag{30}$$

From Eq. (18) and (23), it can be seen that the functions $G[\theta_0(\phi)]$ and $H[\theta_0(\phi)]$ are singular at $\phi=\phi^*$. However, each of $[\theta_0^2(\phi)-\delta^2]G[\theta_0(\phi)]$ and $[(\theta_0^2(\phi)-\delta^2]^{1/2}\times H[\theta_0(\phi)]$ is a regular function for all values of $\phi$. Their limits as $\phi\to\phi^*$ exist and can be found as follows

$$\lim_{\phi\to\phi^*}[\theta_0^2(\phi)-\delta^2]G[\theta_0(\phi)]=\lim_{\phi\to\phi^*}(-A_1)$$
$$=\frac{B_1}{2\delta^2}+\frac{B_2\delta^2}{4} \tag{31}$$

The right-hand side of Eq. (31) is a function of $\gamma$, $\delta$, $M_\infty\delta$, which appears to be quite involved [see Eqs. (20), (21), and (3)]. However, by using a computer to calculate its value for different values of $\gamma$, $M_\infty$, and $M_\infty\delta$, it was found that it is exactly equal to $-\delta$ always. Thus, we may write

$$\lim_{\phi\to\phi^*}[\theta_0^2(\phi)-\delta^2]G[\theta_0(\phi)]=-\delta \tag{32}$$

Similarly, the limit of the other function can be found to be

$$\lim_{\phi\to\phi^*}\sqrt{\theta_0^2(\phi)-\delta^2}\,H[\theta_0(\phi)]=\lim_{\phi\to\phi^*}\sqrt{\theta_0^2(\phi)-\delta^2}\,\ell n[\theta_0(\phi)-\delta]$$
$$=\lim_{\phi\to\phi^*}\frac{\ell n[\theta_0(\phi)-\delta]}{[\theta_0^2(\phi)-\delta^2]^{-1/2}}=0 \tag{33}$$

Using $k(\phi^*)=0$ and the above results in Eq. (29), we find that

$$\theta_1(\phi^*)=1 \tag{34}$$

and Eqs. (27) and (30) show that

$$\Phi(\phi^*)=\delta-\epsilon\cos2\phi^* \tag{35}$$

Since the right-hand side of Eq. (35) is the same as $\theta_c$ at $\phi=\phi^*$ we deduce that

$$\Phi(\phi^*)=\theta_c(\phi^*) \tag{36}$$

i.e., the inlet intersects the cone surface at $\phi=\phi^*$ (also at $\phi=-\phi^*$). Since $z=\ell_1$ can be any cross section of the inlet, we see that the inlet intersects the cone in the lines $\phi=\phi^*$ and $\phi=-\phi^*$ on cone surface. The angle $\phi^*$—fixing the width of the inlet—depends on the function $k(\phi)$, which is still arbitrary and will be chosen later in this section.

We now proceed to fix the slope of the inlet at $\phi=\phi^*$. The functions $k(\phi)$ and $h(\phi)$ will be chosen such that the inlet blends into the cone. First, the function $H(\theta)$ given by Eq. (16) may be written as

$$H(\theta)=\tfrac{1}{2}k_1\ell n(\theta-\delta)+\tfrac{1}{2}k_2\ell n(\theta+\delta)-\tfrac{1}{2}(k_1+k_2)\ell n\theta \tag{37}$$

It is already seen that each of the functions $[\theta_0^2(\phi)-\delta^2]^{1/2}\times H[\theta_0(\phi)]$ and $(\theta_0^2-\delta^2)G[\theta_0(\phi)]$ appearing in the definition of the function $\theta_1(\phi)$ is regular for all values of $\phi$. Therefore, the function $\theta_1(\phi)$ [see Eq. (29)] will be regular for any regular choice of $h(\phi)$. However, in order to make both $\theta_1(\phi)$ and $d\theta_1/d\phi$ regular at $\phi=\phi^*$, we choose $h(\phi)$ such that

$$\frac{k(\phi)h(\phi)}{\sin2\phi k'(\phi)}=k_1\ell n\left[\frac{k(\phi)}{\ell\sqrt{2\delta}}\right]+C_1 \tag{38}$$

where $C_1$ is a constant to be fixed later. The above choice of $h(\phi)$ does not affect the previous results for the points of intersection of the inlet with the cone and will give the required smooth connection with the inlet as we shall see next.

In order to be able to differentiate Eq. (29) and find $d\theta_1/d\phi$, we need to make the following calculations. First, write Eq. (29) in the form

$$\ell_1^2\theta_0(\phi)\theta_1(\phi)=\tan2\phi\;k(\phi)\left\{H[\theta_0(\phi)]\right.$$
$$\left.-\frac{k(\phi)h(\phi)}{\sin2\phi\;k'(\phi)}\right\}-\ell_1^2[\theta_0^2(\phi)-\delta^2]G[\theta_0(\phi)] \tag{39}$$

If $C_1$ is chosen as

$$C_1=-\tfrac{1}{2}(k_1+k_2)\ell n\delta+\tfrac{1}{2}k_2\ell n2\delta$$

then the function

$$H[\theta_0(\phi)]-\frac{k(\phi)h(\phi)}{\sin2\phi k'(\phi)}$$

on the right-hand side of Eq. (39) will become

$$H[\theta_0(\phi)]-\frac{k(\phi)h(\phi)}{\sin2\phi k'(\phi)}=-\frac{1}{2}(k_1+k_2)\ell n\frac{\theta_0(\phi)}{\delta}$$
$$+\frac{1}{2}k_2\ell n\left(\frac{\theta_0(\phi)+\delta}{2\delta}\right)+\frac{1}{2}k_1\ell n\frac{2\delta\ell^2[\theta_0(\phi)-\delta]}{k^2(\phi)} \tag{40}$$

and when $\phi \to \phi^*$ the above equation gives

$$\lim_{\phi \to \phi^*} \left\{ H[\theta_0(\phi)] - \frac{k(\phi)h(\phi)}{\sin 2\phi k'(\phi)} \right\} = k_1 \ell n \left( \frac{\ell}{\ell_1} \right) \tag{41}$$

Now we differentiate Eq. (39) with respect to $\phi$ in order to find the slope of the inlet at $\phi = \phi^*$. We take each of the two terms on the right-hand side and differentiate it separately as follows:

$$\frac{d}{d\phi}\left( \tan 2\phi k(\phi) k'(\phi) \left\{ H[\theta_0(\phi)] - \frac{k(\phi)h(\phi)}{\sin 2\phi k'(\phi)} \right\} \right)$$

$$= \left\{ H[\theta_0(\phi)] - \frac{k(\phi)h(\phi)}{\sin 2\phi k'(\phi)} \right\} [\tan 2\phi k'^2(\phi)$$

$$+ 2 \sec^2 2\phi k(\phi) k'(\phi) + \tan 2\phi k(\phi) k''(\phi)]$$

$$+ \tan 2\phi k(\phi) k'(\phi) \left\{ H'[\theta_0(\phi)] \frac{d\theta_0}{d\phi} - k_1 \frac{k'(\phi)}{k(\phi)} \right\}$$

When $\phi = \phi^*$ we get

$$\frac{d}{d\phi}\left( \tan 2\phi k(\phi) k'(\phi) \left\{ H[\theta_0(\phi)] - \frac{k(\phi)h(\phi)}{\sin 2\phi k'(\phi)} \right\} \right)$$

$$= k_1 \tan 2\phi^* k'^2(\phi^*) \ell n \left( \frac{\ell}{\ell_1} \right)$$

The derivative of the second term can be found by differentiating it term by term and setting $\phi = \phi^*$. The process is lengthy and involved and therefore the details will be omitted. It suffices to give the final result as

$$\frac{d}{d\phi}\left\{ -\ell_1^2 [\theta_0^2(\phi) - \delta^2] G[\theta_0(\phi)] \right\}$$

$$= \tfrac{1}{2} \ell_1 k'(\phi^*)(2A_2 - \delta B_5)$$

$$= \tfrac{1}{2} \ell_1 k'(\phi^*) \left[ 2\left( -\frac{B_4}{\delta^2} - B_3 - \frac{\delta B_5}{2} \right) - \delta B_5 \right]$$

$$= \tfrac{1}{2} \ell_1 k'(\phi^*) \left( -\frac{2}{\delta^2} f_1 b_4 b_5 - \frac{1}{3} f_1 b_4 + 2\delta f_1 b_6 \right)$$

$$= \tfrac{1}{2} \ell_1 k'(\phi^*) \left( -\frac{2 f_1 \delta^2}{3\delta^2 \sqrt{\beta^2 - \delta^2}} - \frac{f_1}{3\sqrt{\beta^2 - \delta^2}} \right.$$

$$\left. + f_1 \frac{1}{\sqrt{\beta^2 - \delta^2}} \right) = 0$$

The derivative of the left-hand side of Eq. (39) is equal to $\delta \ell_1 d\theta_1/d\phi$ at $\phi = \phi^*$. Now by equating the derivatives of the left and the right sides of Eq. (39), we get

$$\left. \frac{d\theta_1}{d\phi} \right|_{\phi = \phi^*} = \frac{k_1}{\delta \ell_1^2} \tan 2\phi^* k'^2(\phi^*) \ell n \left( \frac{\ell}{\ell_1} \right)$$

Thus, the slope of the inlet will be

$$\left. \frac{dH}{d\phi} \right|_{\phi = \phi^*} = 2\epsilon \sin 2\phi^*$$

$$- \epsilon \cos 2\phi^* \left[ \frac{k_1}{\delta \ell_1^2} \tan 2\phi^* k'^2(\phi^*) \ell n \left( \frac{\ell}{\ell_1} \right) \right] \tag{42}$$

From $\theta_c = \delta - \epsilon \cos 2\phi$, the slope of the cone at $\phi = \phi^*$ can be found as

$$\left. \frac{d\theta_c}{d\phi} \right|_{\phi = \phi^*} = 2\epsilon \sin 2\phi^* \tag{43}$$

By comparing Eqs. (42) and (43), we find that the difference in slope between inlet and cone at $\phi = \phi^*$ is given by

$$\left( \frac{d\Phi}{d\phi} - \frac{d\theta_c}{d\phi} \right)_{\phi = \phi^*} = -\epsilon \cos 2\phi^* \frac{k_1}{\delta \ell_1^2} \tan 2\phi^* k'^2(\phi^*) \ell n \frac{\ell}{\ell_1} \tag{44}$$

To have a blended inlet, the difference in slope given above needs to be equal to zero or very small. Except for the conditions set before on the function $k(\phi)$, it is still arbitrary. It is seen from Eq. (44) that the difference in slope between inlet and cone depends on $k'(\phi^*)$. Therefore, to have a blended inlet, we add to the previous conditions on the function $k(\phi)$ the requirement that $k'(\phi^*) = 0$. From Eq. (12), the order of magnitude of the function $k(\phi)$ can be found to be

$$k(\phi) = 0(\ell\delta)$$

Any choice function $k(\phi)$ that satisfies all the conditions set on it will be acceptable. A simple choice is

$$k(\phi) = \ell a \delta \cos^2 \left( \frac{\pi \phi}{2\phi^*} \right) \tag{45}$$

where $a$, $\phi^*$ are arbitrary constants, and $a = 0(1)$.

Summarizing, we have found stream surfaces that intersect the cone in two lines, $\phi = \phi^*$ and $\phi = -\phi^*$. Those stream surfaces are smooth, with no corners, and have the same slope as the cone surface at the line of intersection with the cone.

The above choice of $k(\phi)$ gives a class of inlets of two parameters $a, \phi^*$. The angle $\phi^*$ gives the angular width of the inlet in the cross plane while $a$ determines the inlet thickness

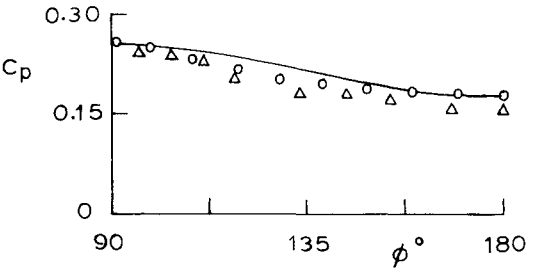


**Fig. 1a Comparison for the coefficient of surface pressure, $M_\infty = 3.09$, $\gamma = 1.4$, $\delta = 0.2904$, $\epsilon/\delta = 0.155$. ——Ref. 5 (analytical), Δ Ref. 10 (experimental), o Ref. 11 (numerical).**

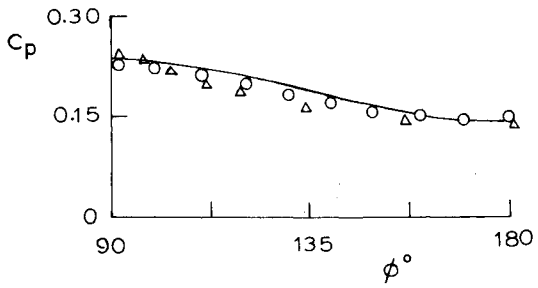


**Fig. 1b Comparison for the coefficient of surface pressure, $M_\infty = 6$, $\gamma = 1.4$, $\delta = 0.2904$, $\epsilon/\delta = 0.155$. ——Ref. 5 (analytical), Δ Ref. 10 (experimental), o Ref. 11 (numerical).**

above the cone. By changing $a,\phi^*$, the rate of mass flow through the inlet can be controlled as we shall see in the following section. It is important to observe that the parameter $a$ needs to be chosen such that all of the inlet lies within the shock layer and is attached to the cone over a reasonable portion fo the rear part of the cone, say, $0.4\ell$–$0.5\ell$. This we shall do in what follows.

In order that all the inlet lies within the shock layer, $a$ needs to be chosen such that

$$\theta_0(\phi) < \beta$$

i.e.,

$$\sqrt{\delta^2 + \left(\frac{\ell a \delta}{\ell_1}\right)^2 \cos^4\left(\frac{\pi\phi}{2\phi^*}\right)} < \sigma\delta$$

The left-hand side of the above inequality will be largest when $\phi = 0$. Using this value and simplifying, we get

$$a < \frac{\ell_1}{\ell}\sqrt{\sigma^2 - 1}$$

i.e.,

$$a = \mu\left(\frac{\ell_1}{\ell}\right)\sqrt{\sigma^2 - 1}, \qquad \mu < 1 \tag{46}$$

For $\mu$ close to 1, the inlet will be attached to the rear part of the cone behind the section $z = \ell_1$, i.e., the inlet length will be $(\ell - \ell_1)$. It is to be noticed that increasing the width of the inlet (i.e., increasing $a$) will decrease the maximum possible length of the inlet $(\ell - \ell_1)$.

In what follows, we find the Newtonian limit of the stream surface that was found before. We find the limiting value of each of $\theta_0(\phi)$ and $\theta_1(\phi)$ as $\gamma \to 1$ and $M_\infty \to \infty$. From Eq. (3a) it can be seen that $\sigma \to 1$ as $\gamma \to 1$ and $M_\infty \to \infty$ and from Eq. (46), $a \to 0$. Equation (45) shows that $k(\phi) \to 0$, and Eq. (28) shows that $\theta_0(\phi) \to \delta$. The first term in the right-hand side of Eq. (39) will approach zero, and we get

$$\lim_{\gamma \to 1, M_\infty \to \infty} \theta_1(\phi) = -\frac{1}{\delta} \lim_{\theta_0 \to \delta} [\theta_0^2(\phi) - \delta^2] G[\theta_0(\phi)]$$

The limit in the right-hand side of the above equation has been found before and its value is equal to one. Thus, we get

$$\Phi(\phi) \to \delta - \epsilon \cos 2\phi \equiv \theta_c$$

i.e., the stream surface approaches the cone surface in the limit $\gamma \to 1$ and $M_\infty \to \infty$ consistent with the Newtonian limit. This completes the design of the inlet, and we can now draw figures to show the results of the above analysis.

First we present in Fig. 1 results and comparisons taken from Ref. 5 for the coefficient of surface pressure. Lee and Rasmussen[5] compared their method with Zakkay and Visich's[10] experimental results and with Martellucci's[11] numerical calculations, for $\gamma = 1.4$, $\delta = 0.2904$, $\epsilon/\delta = 0.155$. In Fig. 1a, $M_\infty = 3.09$, and in Fig. 1b, $M_\infty = 6$. It is seen that although both $\delta$ and $\epsilon/\delta$ are not quite small, the agreement is very good. Since the inlets found in this section are the stream surfaces of the solutions found in Ref. 5, it is expected, in view of the above comparison, that they would compare well with other numerical and experimental works. To the authors' knowledge, such results are not available.

In Figs. 2 and 3, we show inlet cross sections at $z/\ell = 0.5$ and at cone base for $\gamma = 1.4$, $K\delta = 1.2$, and $a = 0.454$, together with the cone and the associated shock wave. Only the lower half of the cone and the shock wave are shown. In Fig. 2, $\phi^* = 50$ deg, $\delta = 0.1$, and $\epsilon/\delta = 0.1$, while in Fig. 3, $\phi^* = 60$ deg, $\delta = 0.2$, and $\epsilon/\delta = 0.15$. It is seen that the inlet has a very smooth cross section and blends very well with the cone surface. Also, by comparing the midsection and the section at the base, we see that the inlet gets closer to the cone surface as we move backward toward the cone base. This is expected in order to have the same mass flow rate through the inlet. Additional figures and tabulated results are given in Ref. 9.

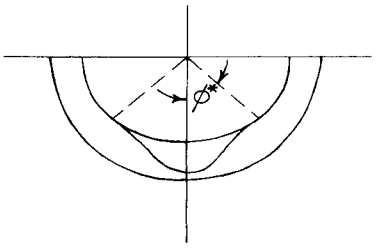


**Fig. 2a Inlet and cone at $z/\ell = 0.5$, $\delta = 0.1$, $\epsilon/\delta = 0.1$, $a = 0.454$, $\phi^* = 50$ deg.**

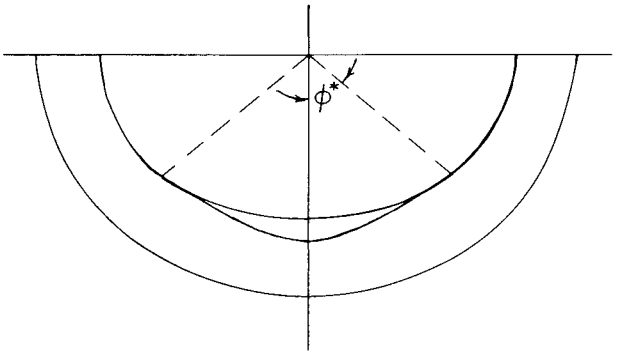


**Fig. 2b Inlet and cone at $z/\ell = 1.0$, $\delta = 0.1$, $\epsilon/\delta = 0.1$, $a = 0.454$, $\phi^* = 50$ deg.**

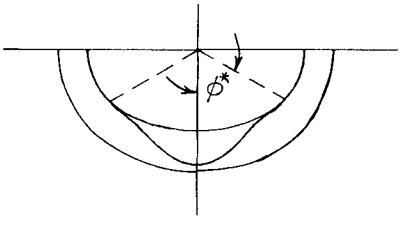


**Fig. 3a Inlet and cone at $z/\ell = 0.5$, $\delta = 0.2$, $\epsilon/\delta = 0.15$, $a = 0.454$, $\phi^* = 60$ deg.**

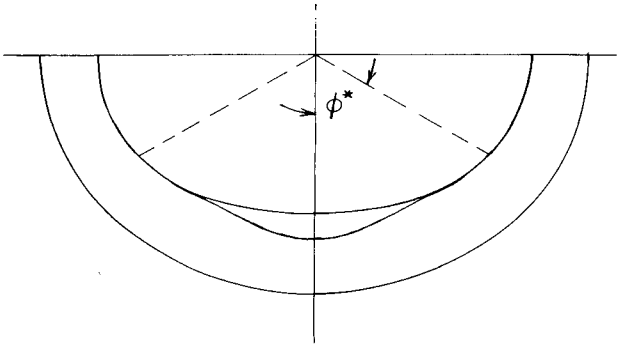


**Fig. 3b Inlet and cone at $z/\ell = 1.0$, $\delta = 0.2$, $\epsilon/\delta = 0.15$, $a = 0.454$, $\phi^* = 60$ deg.**

In the following section we find the rate of mass flow through the inlet. As already seen, the maximum length of the inlet, $\ell - \ell_1$, and inlet thickness controlled by $a$, are inversely proportional to each other. Thus $\ell - \ell_1$ affects the rate of mass flow through the inlet, although all inlets of lengths that are less than $\ell - \ell_1$ and that are parts of that maximum length will have the same mass flow rate because the inlet is a stream surface and the flow is assumed to be inviscid.

## IV. Mass Flow Rate

In this section we calculate the mass flow rate in the inlet. It is obvious that the mass flow rate is an important parameter

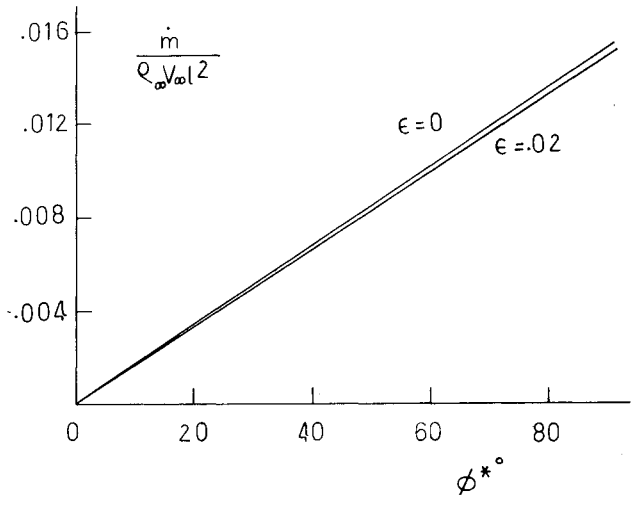


Fig. 4 Variation of $\dot{m}/\rho_\infty V_\infty \ell^2$ with $\phi^*$ and $\epsilon$, $\delta = 0.2$, $a = 0.545$.

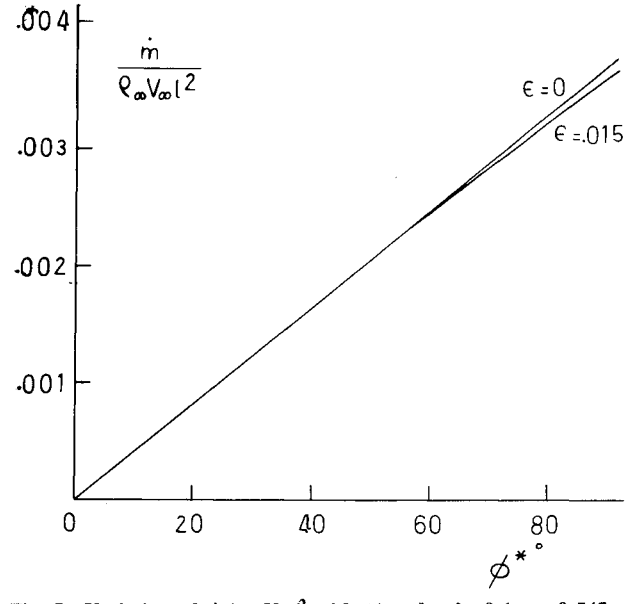


Fig. 5 Variation of $\dot{m}/\rho_\infty V_\infty \ell^2$ with $\phi^*$ and $\epsilon$, $\delta = 0.1$, $a = 0.545$.

because of its direct relation to the waverider thrust force. As mentioned in the previous section, the maximum length of the inlet does affect the maximum possible rate of mass flow through the inlet. The maximum mass flow rate increases as the maximum length decreases. All inlets derived from the maximum length one will have the same rate of mass flow. The geometric parameters $a$, $\phi^*$, the cone parameters $\delta$, $\epsilon$, and the freestream parameters $\gamma$, $M_\infty$ will all affect the rate of mass flow, as we shall now see.

Since the flow through the inlet is inviscid and steady, any cross section $z = \text{const}$ can be used to find $\dot{m}$. We shall use the base section in the following calculations. The fluid velocity in the direction normal to the base is given by

$$V_n = u\cos\theta - v\sin\theta$$

When the approximations used here are introduced into $V_n$, it becomes

$$V_n = u_0(\theta) + \epsilon\cos2\phi U(\theta) - \theta[v_0(\theta) + \epsilon\cos2\phi V(\theta)]$$

The order of magnitude of the functions $u_0$, $U$, $v_0$, $V$ have been found in Sec III. Using those orders of magnitude in $V_n$

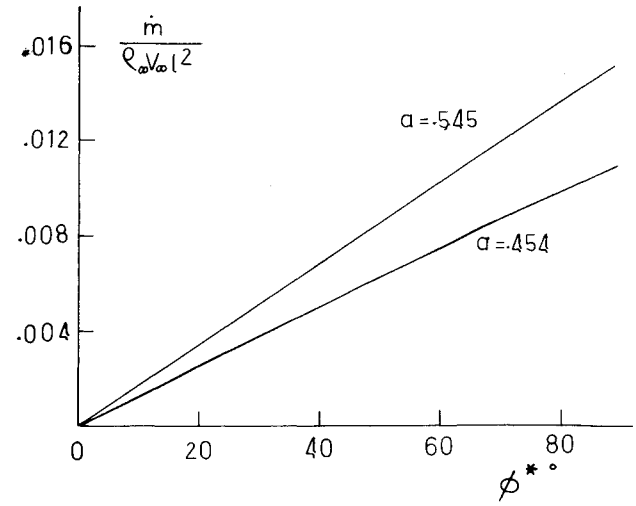


Fig. 6 Variation of $\dot{m}/\rho_\infty V_\infty \ell^2$ with $\phi^*$ and $a$, $\delta = 0.2$, $\epsilon/\delta = 0.1$

and neglecting second order terms in $\delta$, we get

$$V_n = 1 + \epsilon\cos2\phi[U(\theta) - \theta V(\theta)] \tag{47}$$

The density in the flowfield is equal to the density immediately behind the shock wave due to the constant density assumption used. From Ref. 5 we get the following results [Eqs. (3.14)], which will be needed in the following calculations:

$$\frac{\rho_\infty}{\rho_s} = \xi_0 + \epsilon\cos2\phi\xi \qquad \xi_1 = 2g\cot\beta\left(\xi_0 - \frac{\gamma-1}{\gamma+1}\right)$$

$$\xi_0 = \frac{\gamma-1}{\gamma+1} + \frac{2}{(\gamma+1)K_\beta^2} \qquad K_\beta = M_\infty\beta$$

The rate of mass flow $\dot{m}$ will be given by

$$\dot{m} = \int\int \rho_s V_n \mathrm{d}A$$

$$= 2\rho_\infty V_\infty \ell^2 \int_0^{\phi^*} \int_{\theta_c(\phi)}^{H(\phi)} \left\{\frac{1 + \epsilon\cos2\phi[U(\theta) - \theta V(\theta)]}{(\xi_0 + \epsilon_2\cos2\phi\xi_1)}\right\}\theta\,\mathrm{d}\theta\,\mathrm{d}\phi$$

$$= 2\rho_\infty V_\infty \ell^2 \int_0^{\phi^*} \frac{\mathrm{d}\phi}{(\xi_0 + \epsilon\cos2\phi\xi_1)}\left[\frac{\theta^2}{2}\right]_{\delta - \epsilon\cos2\phi}^{\theta_0(\phi) - \epsilon\cos2\phi\theta_1(\phi)}$$

$$+ 2\rho_\infty V_\infty \ell^2 \int_0^{\phi^*} \epsilon\cos2\phi \int_0^{\theta_0} [\theta U(\theta) - \theta^2 V(\theta)]\,\mathrm{d}\theta \tag{48}$$

Terms of order $\epsilon$ in the limits of the second integral have been neglected consistent with the approximations used. Now, let

$$I(\phi) \equiv \int_\delta^{\theta_0(\phi)} [\theta U(\theta) - \theta^2 V(\theta)]\,\mathrm{d}\theta \tag{49}$$

Using the above notations in Eq. (48) and dividing through by $\rho_\infty V_\infty \ell^2$, we get

$$\frac{\dot{m}}{\rho_\infty V_\infty \ell^2} = \int_0^{\phi^*} (\{[\theta_0(\phi) - \epsilon\cos2\phi\theta_1(\phi)]^2$$

$$- (\delta - \epsilon\cos2\phi)^2 + 2\epsilon\cos2\phi I(\phi)\}/(\xi_0 + \epsilon\cos2\phi\xi_1))\mathrm{d}\phi \tag{50}$$

Formulas for $U(\theta)$ and $V(\theta)$ are given in Sec. II. In order to be able to find $I(\phi)$, we first need to write $U(\theta)$ in a convenient from as we have done before for $V(\theta)$. Referring to Eq. (2c) for $U(\theta)$, let

$$\tilde{k}_1 = X(\beta), \qquad \tilde{k}_2 = \frac{X'(\beta)}{4\beta^3}$$

$$k_3 = \frac{1}{\sqrt{\beta^2-\delta^2}}, \qquad k_4 = \frac{\delta^2}{3}$$

$$k_5 = -\frac{1}{2}f_1 k_5, \qquad k_6 = \cos^{-1}\left(\frac{\delta}{\beta}\right), \qquad k_7 = \frac{\beta^2}{6}+\frac{\delta^2}{3}$$

Equation (2c) becomes

$$U(\theta) = \left(\tilde{k}_1 - \tilde{k}_2\beta^4 + \frac{1}{2}k_7 f_1\right)\frac{1}{\theta^2} + \left(\tilde{k}_2 + \frac{1}{2}f_1 k_5 k_6\right)\theta^2 + \frac{5}{12}f_1 k_3\sqrt{\theta^2-\delta^2} - \frac{1}{2}f_1 k_3 k_4\frac{\sqrt{\theta^2-\delta^2}}{\theta^2} - \frac{1}{2}f_1 k_5\theta^2\cos^{-1}\frac{\delta}{\theta} - \frac{1}{2}f_1$$

Further, let

$$K_1 \equiv \tilde{k}_1 - \tilde{k}_2\beta^4 + \frac{1}{2}k_7 f_1, \qquad K_2 \equiv \tilde{k}_1 + \frac{1}{2}f_1 k_5 k_6$$

$$K_3 \equiv \frac{5}{12}f_1 k_3, \qquad K_4 \equiv -\frac{1}{2}f_1 k_3 k_4$$

$$K_5 \equiv -\frac{1}{2}f_1 k_5, \qquad K_6 \equiv -\frac{1}{2}f_1$$

Thus $U(\theta)$ becomes

$$U(\theta) = \frac{K_1}{\theta} + K_2\theta^2 + K_3\sqrt{\theta^2-\delta^2} + K_4\frac{\sqrt{\theta^2-\delta^2}}{\theta^2} + K_5\theta^2\cos^{-1}\frac{\delta}{\theta} + K_6 \tag{51}$$

Using Eqs. (2d) and (51) in Eq. (49); the latter may be written as

$$I(\phi) = \int_\delta^{\theta_0(\phi)}\left[\frac{C_0}{\theta} + C_2\theta^3 + C_2\theta\sqrt{\theta^2-\delta^2} + C_4\frac{\sqrt{\theta^2-\delta^2}}{\theta} + C_5\theta^3\cos^{-1}\frac{\delta}{\theta} + C_6\theta\right]d\theta \tag{52}$$

where

$$C_0 = K_1 - B_1, \qquad C_2 = K_2 - B_2, \qquad C_3 = K_3 - B_3$$

$$C_4 = K_4 - B_4, \qquad C_5 = K_5 - B_5, \qquad C_6 = K_6$$

Each of the integrals in Eq. (52) can be easily found. The final result is

$$I(\phi) = C_0\ell n\frac{\theta_0(\phi)}{\delta} + \frac{C_2}{4}[\theta_0^4(\phi)-\delta^4] + \frac{C_3}{3}[\theta_0^2(\phi)-\delta^2]^{3/2} + C_4\sqrt{\theta_0^2(\phi)-\delta^2} - \delta C_4\cos^{-1}\frac{\delta}{\theta_0(\phi)} + \frac{C_6}{2}[\theta_0^2(\phi)-\delta^2] + \frac{C_5}{4}\theta_0^4(\phi)\cos^{-1}\frac{\delta}{\theta_0(c)} - \frac{C_5}{12}\delta^4\sqrt{1-[\delta^2/\theta_0^2(\phi)]}\left\{\left[\frac{\theta_0(\phi)}{\delta}\right]^3 + \frac{2\theta_0(\phi)}{\delta}\right\}$$

Having found $I(\phi)$ in closed form, $\dot{m}$ can be easily found from Eq. (50) by numerical quadrature using a computer.

Results of $\dot{m}/\rho_\infty V_\infty \ell^2$ vs $\phi^*$ for various values of $\delta$, $\epsilon$, and $a$ are shown in Figs. 4–6. It is seen that $\dot{m}$ increases with increasing $\phi^*$, as is expected. Figure 4 shows that $\dot{m}$ decreases slightly when $\epsilon$ increases, while Fig. 5 shows that $\dot{m}$ remains almost unchanged for $\phi^*$ up to 60 deg, then decreases slightly. The effect of $\epsilon$ on $\dot{m}$ is seen to be small and less than 5% in all cases. Figure 6 shows the effect of the parameter $a$ on the rate of mass flow. It is seen that $\dot{m}$ increases significantly when $a$ increases. This result is also expected since increasing $a$ increases the area of the inlet. The results of $\dot{m}/p_\infty V_\infty \ell^2$ vs $\phi^*$ at $\epsilon = 0$ show a straight-line relation. In this special case, Eq. (50) reduces to

$$\frac{\dot{m}}{\rho_\infty V_\infty \ell^2} = \frac{1}{\xi_0}\int_0^{\phi^*}[\theta_0^2(\phi)-\delta^2]\,d\phi = \frac{1}{\xi_0}\left(\frac{a\delta}{\ell_1/\ell}\right)^2\int_0^{\phi^*}\cos^4\frac{\pi\phi}{2\phi^*}\,d\phi = \frac{3\phi^*}{8\xi_0}\left(\frac{a\delta}{\ell_1/\ell}\right)^2$$

which gives a linear relation between $\dot{m}$ and $\phi^*$, exactly as the results illustrate.

## V. Concluding Remarks

By use of a simple and systematic approach, the stream surfaces of the elliptic-cone flow at zero angle of attack have been found in closed form and used to design smooth blended inlets which can be attached to the waverider configuration proposed in Ref. 2. The rate of mass flow through these inlets has also been found in closed form. The results can be used in the hypersonic Mach number range for which $K\delta$ is 0(1) or larger.

The analysis is based on the assumptions of steady inviscid flow at the design point of the elliptic-cone flow, with the basic goal of achieving a high lift-to-drag ratio over a reasonable range of conditions. It is therefore desirable to compare the present results with experiment and to establish the actual performance of these inlets compared with other designs.

The inlet has been assumed to be very thin so that its presence does not affect the cone flowfield. Account of the real situation of finite wall thickness and other disruption of the flow pattern caused by the combustion process taking place in the inlet needs to be considered.

The method used here can also be used for the other waverider configuration given in Ref. 2 derived from circular-cone flow at small angles of attack and, in general, can be useful in other similar situations in which stream surfaces of a flowfield need to be found.

## Acknowledgments

This work was sponsored by the U.S. Air Force, Air Force Armament Laboratory, under Contract FO-8635-80-K-0304.

## References

[1]Kuchemann, D., "Hypersonic Aircraft and Their Aerodynamic Problems," *Progress in Aeronautical Sciences,* Vol. 6, Pergamon, London, 1965, p. 271.

[2]Rasmussen, M.L., "Lifting Bodies Derived from Supersonic Flows Past Inclined Circular and Elliptic Cones," School of Aerospace, Mechanical, and Nuclear Engineering, University of Oklahoma, Reseach Rept. OU-AMNE-78-11, 1978.

[3]Rasmussen, M.L., "Waverider Configuration Derived from Inclined Circular and Elliptic Cones," *Journal of Spacecraft and Rockets,* Vol. 17, June 1980, pp. 537-545.

[4]Lanham, D.L., "Static Force, Pressure, Oil Flow Visualization Tests of Supersonic Aerodynamic Lifting Bodies at Mach Numbers 3 to 5," Arnold Engineering Development Center, U.S. Air Force, Feb. 1980.

[5]Lee, H.M. and Rasmussen, M.L.,"Hypersonic Flow Past a Slender Elliptic Cone," School of Aerospace, Mechanical, and Nuclear Engineering, University of Oklahoma, Research Rept. OU-AMNE-78-2, 1978.

[6]Chapkis, R.T., "Hypersonic Flow over an Elliptic Cone: Theory and Experiment," *Journal of the Aeronautical Sciences,* Vol. 28, No. 11, 1961, pp. 844-854.

[7]Melnik, R.E., "Vortical Singularities in Conical Flow," *AIAA Journal,* Vol. 5, April 1967, pp. 631-637.

[8]Cheng, H.K., "Hypersonic Flows Past a Yawed Circular Cone and other Pointed Bodies," *Journal of Fluid Mechanics,* Vol. 12, 1962, pp. 169-191.

[9]Hemdan, H.T., and Jischke, M.C., "Inlets for Waveriders Derived from Elliptic Cone Streamsurfaces," School of Aerospace, Mechanical, and Nuclear Engineering, University of Oklahoma, Research Rept. OU-AMNE-81-6, 1981.

[10]Zakkay, V. and Visich, M. Jr., "Experimental Pressure Distribution on Conical Elliptic Bodies at $M_\infty = 3.09$ and 6.0," Polytechnic Institute of Brooklyn, PIBL Rept. 467, March 1959.

[11]Martellucci, A., "An Extension of the Linearized Characteristics Method for Calculating the Supersonic Flow Around Elliptic Cones," *Journal of the Aeronautical Sciences,* Vol. 27, No. 9, 1960, pp. 667-674.